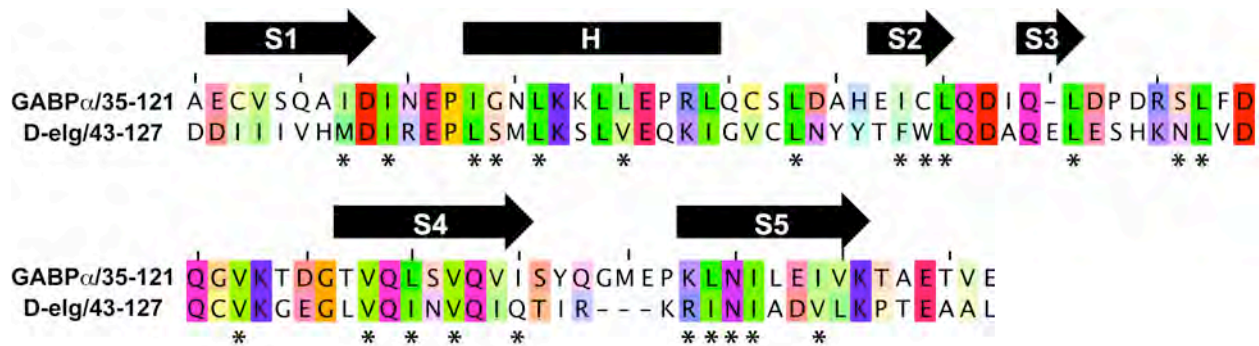


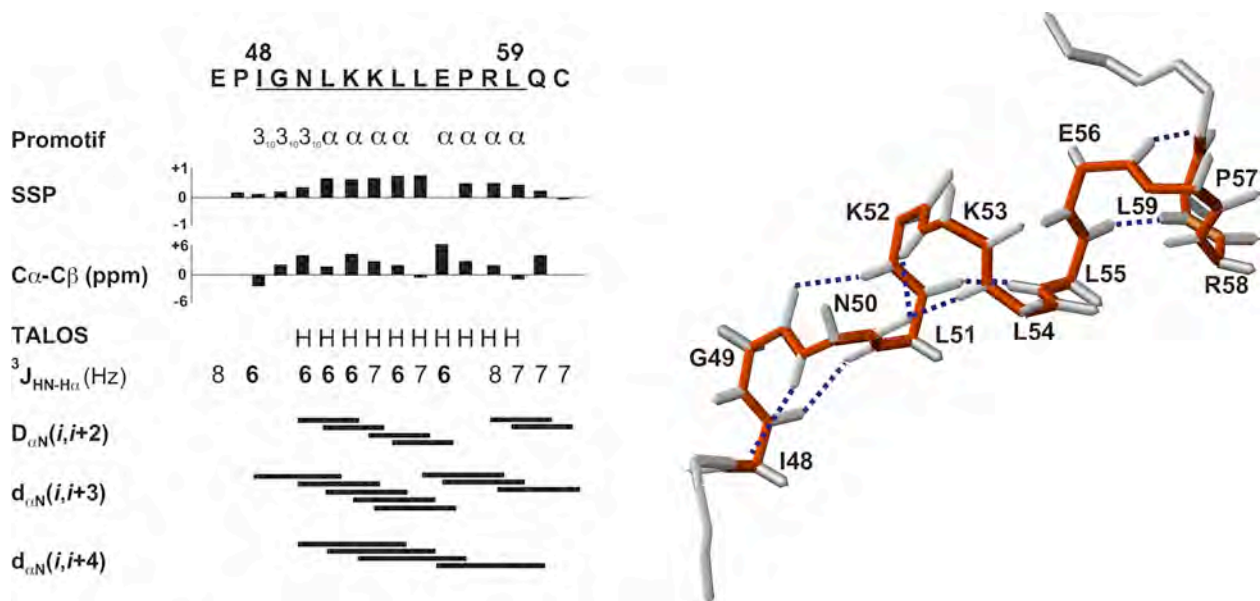
## SUPPLEMENTAL MATERIAL

**Supplemental Figure S1:**



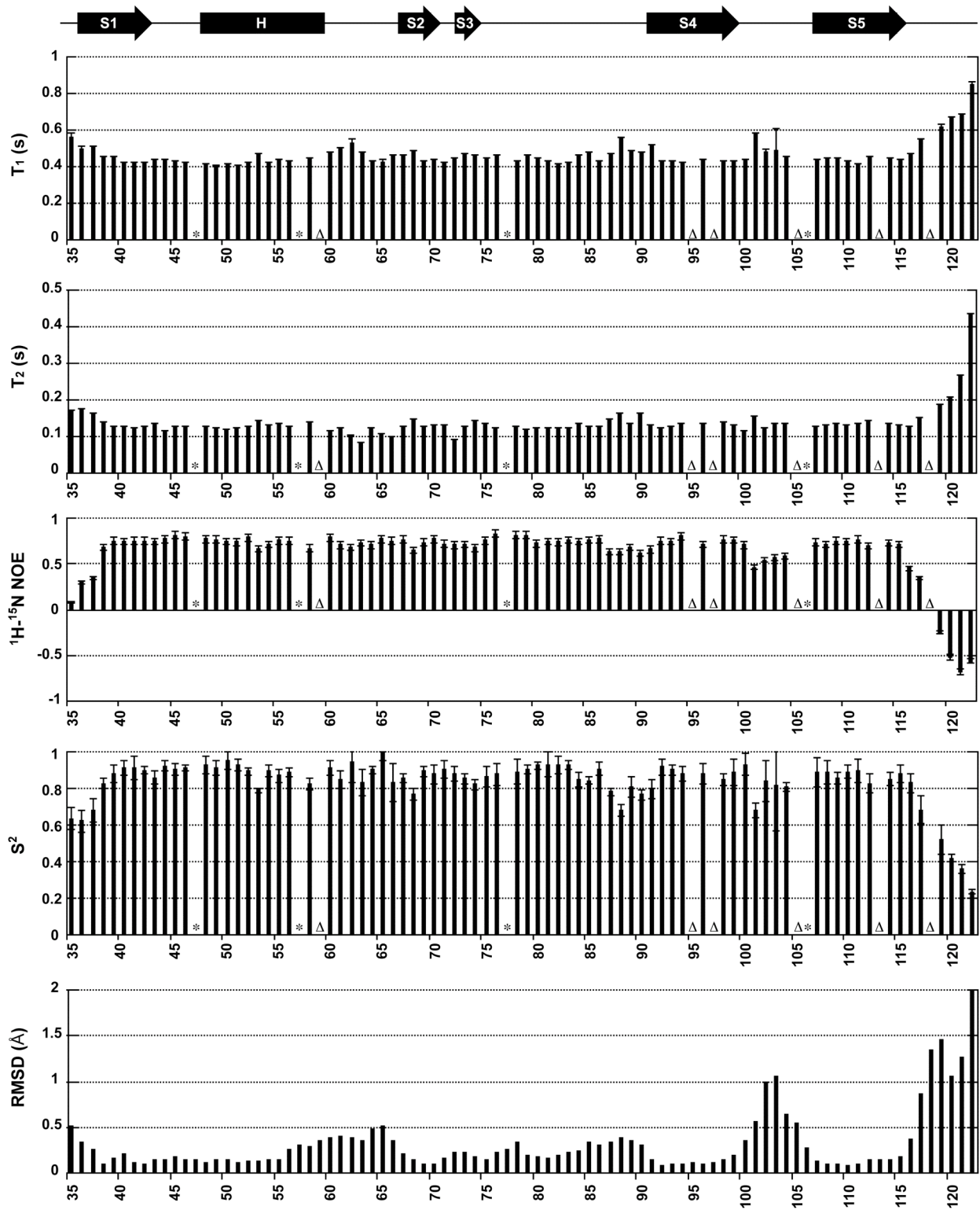
Sequence alignment of murine GABP $\alpha$ <sup>35-121</sup> with the corresponding region in the apparent GABP $\alpha$  ortholog in *Drosophila melanogaster* Elg, generated with CLUSTAL X<sup>1</sup> and Jalview.<sup>2</sup> Residues are colored by physicochemical properties according to the Taylor scheme.<sup>2</sup> The helix and  $\beta$ -strands of the OST domain are indicated along with core hydrophobic residues (\*) having side-chain with accessible surface areas less than 10% of a random coil polypeptide, as calculated by VADAR.<sup>3</sup> Note that other sequenced GABP $\alpha$  orthologs (23 vertebrate genes) have highly conserved sequences throughout the domain and thus are not shown for clarity.

### Supplemental Figure S2:



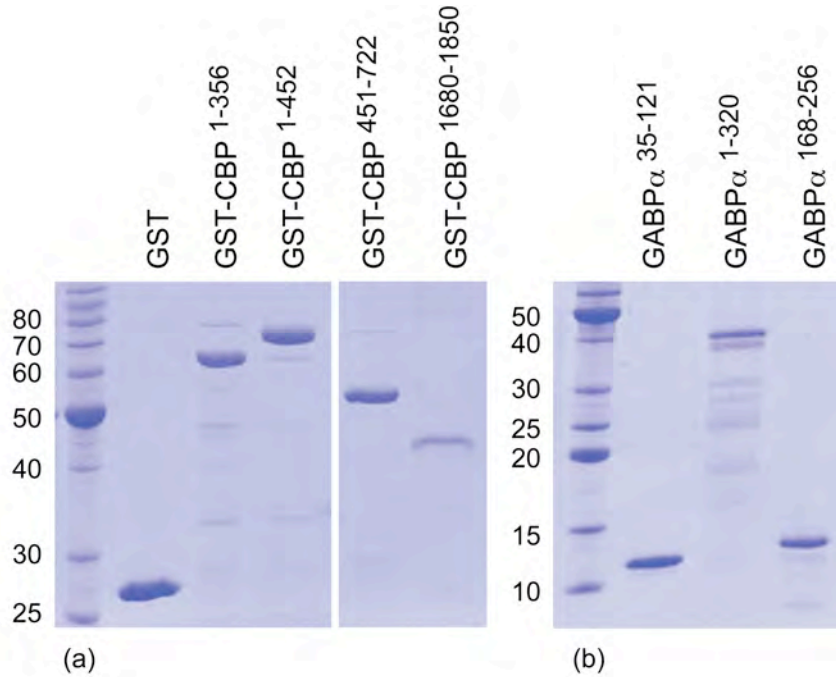
Residues (48-59) in the GABP $\alpha$ <sup>35-121</sup> OST domain adopt a 3<sub>10</sub> helical conformation followed by a distorted  $\alpha$ -helical conformation, as defined by Promotif.<sup>4</sup> The 3<sub>10</sub> helix was identified based on the inferred hydrogen bonds (dashed line) between P47/N50 and I48/L51 ( $\text{CO}_i\text{-H}^{\text{N}}_{i+3}$ ) in the structural ensemble. Furthermore,  $\text{H}^{\alpha}_i\text{-H}^{\text{N}}_{i+4}$  NOE interactions, diagnostic of a regular  $\alpha$ -helix, appear only after N50. The helix is kinked near P57 due to the absence of hydrogen bonds between the residues preceding (E56) and following (R58) the proline to K52 and L54, respectively. The regular geometry of the  $\alpha$ -helix is regained after R58 indicated by with L55/L59 and E56/Q60 hydrogen bonds. The helical nature of this region is confirmed experimentally by three criteria: (1) analysis of main chain  $^1\text{H}^{\text{N}}$ ,  $^{15}\text{N}$ ,  $^{13}\text{C}^{\alpha}$ ,  $^{13}\text{C}^{\beta}$ , and/or  $^{13}\text{C}^{\gamma}$  chemical shifts using the algorithms SSP<sup>5</sup> (scores 0 to +1 indicating increasing helical character) and TALOS<sup>6</sup> (H for predicted  $(\Phi, \Psi)$  angles characteristic of helices), as well patterns of ( $^{13}\text{C}^{\alpha}$ - $^{13}\text{C}^{\beta}$ ) shift differences relative to random coil values (+ differences indicate a helical conformation); (2)  $^3J_{\text{HN-H}\alpha}$  coupling constants (< 6 Hz for a helix); and (3) short-range NOE patterns between  $\text{H}^{\text{N}}$  and  $\text{H}^{\alpha}$  nuclei.<sup>7</sup> Note that numerous examples of prolines with helices have been documented, yielding similar conformational changes as observed for the OST domain.<sup>8</sup>

Supplemental Figure S3:



Dynamic characterization of the GABP $\alpha$  OST domain. Shown are backbone (a-c)  $^{15}\text{N}$ -  $T_1$ ,  $T_2$ , and heteronuclear  $^1\text{H}$ - $^{15}\text{N}$  NOE relaxation parameters, along with (d) fit anisotropic model free order parameter  $S^2$ . (e) Also shown are the root-mean-square deviations of backbone heavy atoms of the GABP $\alpha$ <sup>35-121</sup> structural ensemble relative to the average structure, after superimposition of ordered residues (Table 1). Decreasing NOE and  $S^2$  values indicate increasing mobility on the nsec-psec time scale. Prolines and the unresolved amide signals (L59, S95, Q97, E105, I113, E118) in the  $^1\text{H}$ - $^{15}\text{N}$  HSQC spectrum are indicated as \* and  $\Delta$ , respectively. Methods: Amide  $^{15}\text{N}$  relaxation parameters were acquired at 500 MHz as described previously.<sup>9</sup> Data were processed with NMRpipe<sup>10</sup> and fit to a single exponential decay using Sparky<sup>11</sup> to obtain the  $T_1$  and  $T_2$  lifetimes. Anisotropic diffusion and model-free order parameters ( $S^2$ ) were calculated with Tensor 2.0 using the lowest energy structural model of GABP $\alpha$ <sup>35-121</sup>.<sup>12</sup> Residues showing fast internal motions or chemical exchange broadening were excluded from the diffusion tensor calculations.<sup>13</sup> Global displacements for the backbone heavy atoms in the structural ensemble were calculated using MolMol.<sup>14</sup>

**Supplemental Figure S4:**



Analysis of the purified (a) GST-CBP and (b) GABP $\alpha$  fragments by reducing 10% and 15% SDS-PAGE with Coomassie staining, respectively. Each sample was 2  $\mu$ g, except for 0.5  $\mu$ g of GST-CBP<sup>1680-1850</sup>. These proteins were used for the GST-pulldown assays presented in Figure 4(f-h). Molecular mass markers (kDa) are resolved in the left lane of each panel.

## SUPPLEMENTAL REFERENCES

1. Chenna, R., Sugawara, H., Koike, T., Lopez, R., Gibson, T. J., Higgins, D. G. & Thompson, J. D. (2003). Multiple sequence alignment with the Clustal series of programs. *Nuc. Acids Res.* **31**, 3497-3500.
2. Clamp, M., Cuff, J., Searle, S. M. & Barton, G. J. (2004). The Jalview Java alignment editor. *Bioinformatics* **20**, 426-427.
3. Willard, L., Ranjan, A., Zhang, H. Y., Monzavi, H., Boyko, R. F., Sykes, B. D. & Wishart, D. S. (2003). Vadar: A web server for quantitative evaluation of protein structure quality. *Nuc. Acids Res.* **31**, 3316-3319.
4. Hutchinson, E. G. & Thornton, J. M. (1996). Promotif - a program to identify and analyze structural motifs in proteins. *Prot. Sci.* **5**, 212-220.
5. Marsh, J. A., Singh, V. K., Jia, Z. C. & Forman-Kay, J. D. (2006). Sensitivity of secondary structure propensities to sequence differences between alpha- and gamma-synuclein: Implications for fibrillation. *Prot. Sci.* **15**, 2795-2804.
6. Cornilescu, G., Delaglio, F. & Bax, A. (1999). Protein backbone angle restraints from searching a database for chemical shift and sequence homology. *J. Biomol. NMR* **13**, 289-302.
7. Wüthrich, K. (1986). *NMR of Proteins and Nucleic Acids*. J. Wiley & Sons.
8. Barlow, D. J. & Thornton, J. M. (1988). Helix geometry in proteins. *J. Mol. Biol.* **201**, 601-619.
9. Farrow, N. A., Muhandiram, R., Singer, A. U., Pascal, S. M., Kay, C. M., Gish, G., Shoelson, S. E., Pawson, T., Forman-Kay, J. D. & Kay, L. E. (1994). Backbone dynamics of a free and phosphopeptide-complexed Src homology 2 domain studied by  $^{15}\text{N}$  NMR relaxation. *Biochemistry* **33**, 5984-6003.
10. Delaglio, F., Grzesiek, S., Vuister, G. W., Zhu, G., Pfeifer, J. & Bax, A. (1995). NMRpipe - a multidimensional spectral processing system based on Unix pipes. *J. Biomol. NMR* **6**, 277-293.
11. Goddard, T. D. & Kneller, D. G. Sparky 3, University of California, San Francisco.
12. Dosset, P., Hus, J. C., Blackledge, M. & Marion, D. (2000). Efficient analysis of macromolecular rotational diffusion from heteronuclear relaxation data. *J. Biomol. NMR* **16**, 23-28.
13. Tjandra, N., Kuboniwa, H., Ren, H. & Bax, A. (1995). Rotational dynamics of calcium-free calmodulin studied by N-15 NMR relaxation measurements. *Eur. J. Biochem.* **230**, 1014-1024.
14. Koradi, R., Billeter, M. & Wüthrich, K. (1996). MolMol: A program for display and analysis of macromolecular structures. *J. Mol. Graph.* **14**, 51-55.